

We are IntechOpen, the world's leading publisher of Open Access books Built by scientists, for scientists

6,900

Open access books available

186,000

International authors and editors

200M

Downloads

Our authors are among the

154

Countries delivered to

TOP 1%

most cited scientists

12.2%

Contributors from top 500 universities



WEB OF SCIENCE™

Selection of our books indexed in the Book Citation Index
in Web of Science™ Core Collection (BKCI)

Interested in publishing with us?
Contact book.department@intechopen.com

Numbers displayed above are based on latest data collected.
For more information visit www.intechopen.com



Mechanical and Structural Behavior of Swelling Elastomers under Compressive Loading

Sayyad Zahid Qamar, Maaz Akhtar and Tasneem Pervez

The history of science shows that theories are perishable. With every new truth that is revealed we get a better understanding of Nature and our conceptions and views are modified.

Nikola Tesla

Abstract

Swelling elastomers are a new breed of advanced polymers, and found increasing use in drilling of difficult oil and gas wells. It is important to know how an elastomer will behave under a given set of well conditions, especially after the initial quick-swell period. Good design depends on appropriate material selection. Results are presented in this chapter from experimental and numerical studies conducted to analyze how compressive and bulk behavior of actual oilfield elastomers changes due to swelling. Six key attributes of swelling elastomers needed for design improvement and performance analysis of elastomer seals are discussed: four mechanical properties (elastic modulus E , bulk modulus K , shear modulus G , and Poisson's ratio ν), and two polymer structure characteristics (cross-link chain density N_C , and average molecular weight M_C). These parameters were experimentally determined before and after various stages of swelling for two different swelling elastomers being currently used by the regional petroleum industry, in low and high salinity brines. To strengthen the experimental results, and to be able to forecast for other elastomer materials and well conditions, tests were also simulated using the commercial FEM package ABAQUS, using the best available hyperelastic material models.

Keywords: swelling elastomer, compressive loading, mechanical testing, elastomer structure

1. Introduction

As discussed earlier, swelling elastomers are a new breed of advanced polymers [1]. Over the last two decades, they have found increasing use in drilling of difficult oil and gas wells, remediation of damaged wells, and renewal of production from abandoned wells [2–8]. It is important to know whether an elastomer type or a certain seal design will function properly and reliably under a given set of well conditions [9]. Investigation of the swelling and mechanical behavior of these elastomers is essential in resolving application and design issues. When an

elastomer seal is positioned in the well, environmental conditions initiate the swelling. The material may continue to swell throughout its life, though very slowly after the initial quick-swell period [10, 11]. Swelling results in changes in its mechanical properties and sealing response. If elastomer seals are put into use without thoroughly studying these changes, seal failure can happen in certain cases, causing loss of time, money, and other resources. Rework is not only time consuming but at times not possible at all. Failures may even cause the production from the well to stop.

One critical aspect of good design is appropriate material selection. This cannot be done without reliable knowledge of how the material will behave when exposed to different loads, temperatures, and other environmental conditions. As swelling elastomers are basically used as sealing elements in petroleum applications, and as seals are mostly under compressive loading, investigation of the mechanical behavior of elastomers under compression is very important. Contemporary elastomer seal design is usually based on laboratory tests and trial-and-error method. Testing under all possible combinations of field parameters (elastomer material, water salinity, oil type, temperature, pressure, etc) in the laboratory is almost impossible, especially for extended swelling periods. Numerical modeling and simulation of seal design, validated by experimental results, may provide answers for possible scenarios, which cannot be attempted experimentally. Numerical simulations can shorten the lead time for development of robust sealing applications in difficult or new oil and gas wells, offering an accurate and cost effective alternative to extensive testing.

Results are presented in this chapter from experimental and numerical studies conducted to analyze how compressive and bulk behavior of actual oilfield elastomers changes due to swelling. Six key attributes of swelling elastomers needed for design improvement and performance analysis of elastomer seals are discussed: four mechanical properties (elastic modulus E , bulk modulus K , shear modulus G , and Poisson's ratio ν), and two polymer structure characteristics (cross-link chain density N_C , and average molecular weight M_C). These parameters were experimentally determined before and after various stages of swelling for two different swelling elastomers being currently used by the regional petroleum industry, in low and high salinity brines. To strengthen the experimental results, and to be able to forecast for other elastomer materials and well conditions, tests were also simulated [12] using the commercial FEM package ABAQUS [13], using the best available hyperelastic material models.

2. Mathematical background

As stated above, this chapter describes the effect of swelling on mechanical properties (macro-level behavior) and polymer structure (micro-level characteristics) of two elastomers under compressive loading. Brief theoretical background and inter-relationships of these quantities are presented in this section.

2.1 Macroscopic behavior: isotropic relationships

The elastic behavior of any isotropic material is completely described by Hooke's law [14]:

$$\varepsilon_x = \frac{1}{E} [\sigma_x - \nu(\sigma_y + \sigma_z)]$$

$$\begin{aligned}\varepsilon_y &= \frac{1}{E} [\sigma_y - \nu(\sigma_z + \sigma_x)] \\ \varepsilon_z &= \frac{1}{E} [\sigma_z - \nu(\sigma_x + \sigma_y)],\end{aligned}\quad (1)$$

where σ is the engineering stress and ε is the strain. Being in the elastic region, engineering shear strain (γ) is obviously proportional to shear stress (τ):

$$\gamma_{yz} = \frac{1}{G} \tau_{yz}, \gamma_{zx} = \frac{1}{G} \tau_{zx}, \gamma_{xy} = \frac{1}{G} \tau_{xy}\quad (2)$$

Figure 1 shows a body under a state of pure shear and its Mohr circle representation giving the principal stresses.

$$\sigma_1 = \tau_{xy}, \quad \sigma_2 = -\tau_{xy}, \quad \sigma_3 = 0, \quad \tau_{12} = 0\quad (3)$$

We can use Hooke's law Eq. (1) to find the principal strains:

$$\varepsilon_1 = \frac{\tau_{xy}(1 + \nu)}{E}, \quad \varepsilon_2 = -\frac{\tau_{xy}(1 + \nu)}{E}.\quad (4)$$

Shear strain γ_{xy} can also be expressed in terms of the principal strains:

$$\gamma_{xy} = \varepsilon_1 - \varepsilon_2 = \frac{2\tau_{xy}(1 + \nu)}{E}\quad (5)$$

Comparing Eqs. (2) and (5), shear modulus becomes:

$$G = \frac{E}{2(1 + \nu)}.\quad (6)$$

Bulk modulus (K) is related to volume dilatation (volumetric strain) $\delta = \Delta V/V$ and hydrostatic pressure $p = \frac{1}{3}(\sigma_x + \sigma_y + \sigma_z)$:

$$\delta = -\frac{p}{K}.\quad (7)$$

For a body undergoing linear strains, it can be easily shown that [15].

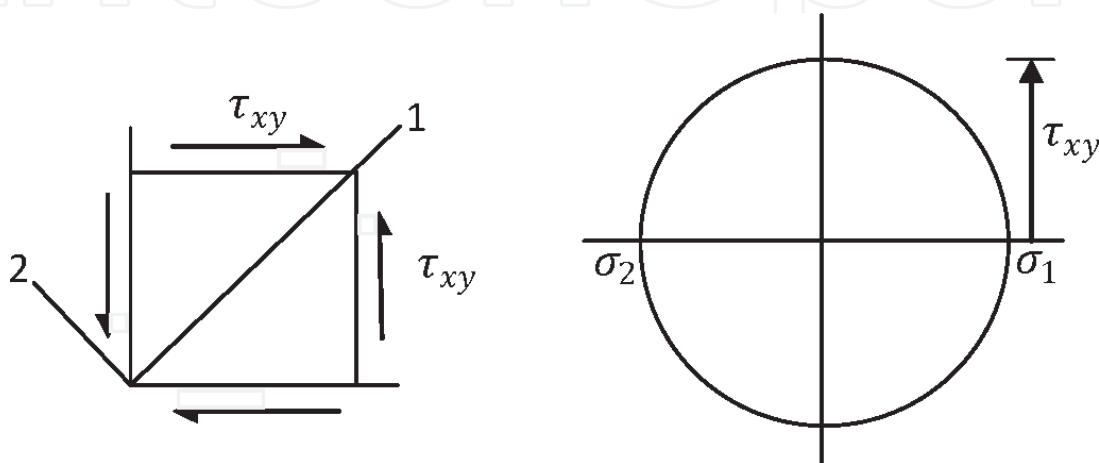


Figure 1.
 A body under state of pure shear and its Mohr circle representation.

$$\frac{dV}{V} = d\varepsilon_x + d\varepsilon_y + d\varepsilon_z. \quad (8)$$

Combining Eqs. (7) and (8), volume dilatation can be expressed as

$$\delta = \varepsilon_x + \varepsilon_y + \varepsilon_z. \quad (9)$$

Comparing this result with Eq. (1), and simplifying, we get

$$\delta = \left(\frac{1 - 2\nu}{E} \right) (\sigma_x + \sigma_y + \sigma_z). \quad (10)$$

Recalling the definition of hydrostatic pressure p , and comparing with Eq. (7), the relationship between bulk modulus and Poisson's ratio comes out to be

$$K = \frac{E}{3(1 - 2\nu)}. \quad (11)$$

Once the values of E and K are established experimentally, shear modulus (G) and Poisson's ratio (ν) can be determined using the isotropic relations Eqs. (6) and (11).

2.2 Structural behavior

Chemical and physical structure of a polymer is modified at different stages of swelling. The resulting changes in structural behavior affect the performance of swelling elastomer seals. It is important, therefore, to understand the factors that can affect swelling elastomer structure and, hence, its properties. Current section discusses the method of determining major structural properties.

2.2.1 Chain density

For any rubber-like material, network strands are formed both by cross-linking and by molecular entanglement. As the degree of cross-linking increases, the cross-link chain density increases, making the elastomer more rigid, thus giving higher values of stiffness and shear modulus G [16]. Chain density can therefore be used as a measure of the swelling capability of an elastomer. For elastomers subjected to small strains, shear modulus is directly related to the number of cross-link chains per unit volume N_c [17]:

$$G = N_c k T, \quad (12)$$

where k is the Boltzmann's constant, and T is the temperature in Kelvins.

2.2.2 Number average chain molecular weight

Length of the network chain decreases due to an increase in the degree of cross-linking. In any polymer, chain density is closely related to the average molecular weight, and this property can also be used to explain the mechanics of swelling [17]. Multiplying and dividing Eq. (12) by Avogadro's number N_A , and recalling that $R = N_A k$, we can obtain

$$G = \frac{N_c RT}{N_A}. \quad (13)$$

If n is the number of chains, Avogadro's number can also be written as

$$N_A = nM_c/m. \quad (14)$$

Combining the definition of chain density ($N_c = n/V$) with Eq. (14) yields

$$N_c/N_A = \rho/M_c. \quad (15)$$

Comparing this result with Eq. (13), we can get the expression for the number average chain molecular weight

$$M_c = \rho RT/G. \quad (16)$$

Once the value of shear modulus G is determined, these structural properties of the elastomer (N_c and M_c) can be easily evaluated using Eqs. (12) and (16).

3. Experimental work

Various researchers have investigated the behavior of rubber-like materials under compression [16], but not for swelling elastomers. The main objective of experiments described here is to obtain swelling behavior, stress-strain, and pressure-volumetric strain curves. Curve fitting on the linear portions of these graphs determines the values of elastic and bulk moduli. These curves are also used to extract material coefficients for the hyperelastic models used for numerical simulations.

Samples of two different water-swelling elastomers were allowed to swell for a one month period in saline water of 6,000 ppm (0.6%) and 120,000 ppm (12%) concentrations at 50°C; actual field conditions in regional oil-wells. Samples were placed in sealable glass jars containing the swelling medium and identified by mnemonic code names. Jars were placed inside servo-controlled ovens maintained at 50°C temperature throughout the thirty days test period. Compression and bulk tests were carried out on disc samples before swelling and after 1, 2, 4, 7, 10, 16, 23, and 30 days of swelling. To ensure repeatability and consistency, all reported values are average of readings from three samples.

3.1 Swelling tests

Cutting of disc samples and preparation of salt solutions has been described in detail in Chapter 3. Procedure for swelling tests is given below.

3.1.1 Test procedure

Samples were placed in sealable glass jars containing proper swelling medium and identified by mnemonic codenames. Jars were placed inside servo-controlled ovens maintained at 50°C temperature throughout the 30-day test period. Volume, thickness, mass, and hardness of each sample was measured before swelling and after different days of swelling. Test setup has been described in Chapter 3. Mass was measured using a digital balance. Volume measurements were done by a specially constructed (in-house) graduated beaker-cylinder arrangement based on the

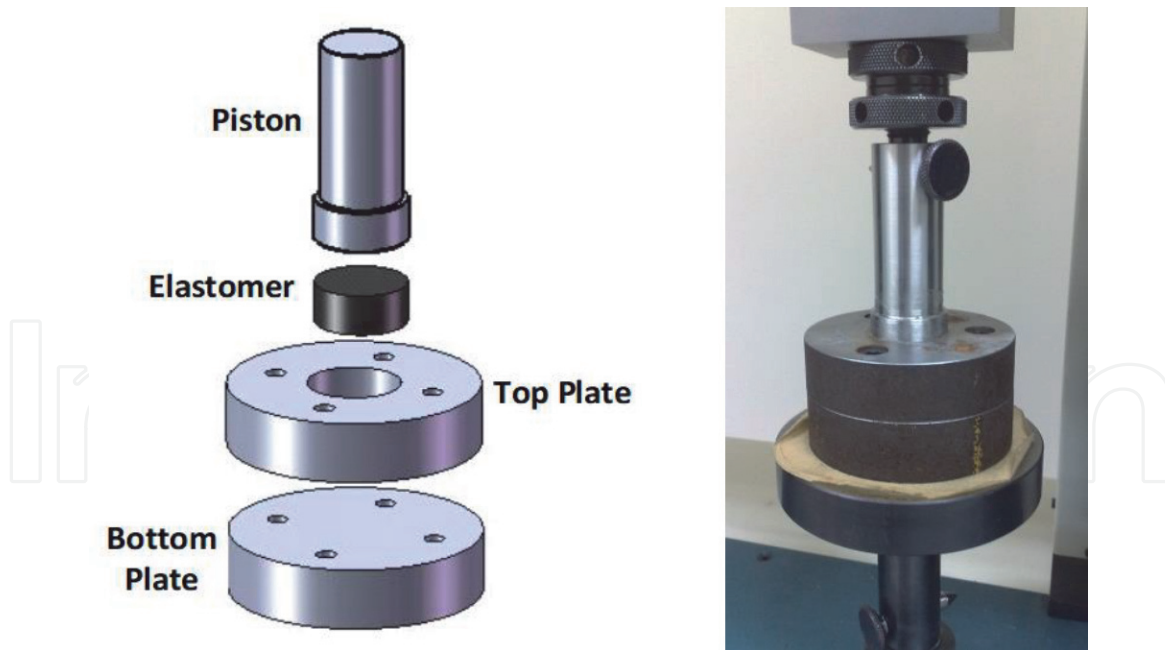


Figure 2.
Designed and fabricated test rig for bulk experiments.

displacement method. Thickness measurements were carried out using digital Vernier calipers. Hardness readings were taken using a scale-A durometer.

3.2 Compression testing

Compression tests are performed in accordance with ASTM-D575 standard test method [18] as described in detail in Chapter 6.

3.3 Bulk testing

No standard is available for bulk testing of elastomers. A special test rig was therefore designed and fabricated in-house for bulk experiments; **Figure 2**. The rig was designed in such a way that under compressive loading the specimen is constrained to move only in the axial direction and radial expansion is not allowed. To match with compression testing, load is applied at the rate of 12 mm/min until the specimen fails. Force-deformation results are recorded and later converted into pressure-volumetric strain data.

4. Numerical investigation

Just as in experiments, simulations are run before swelling and after every swelling period. Using the commercial finite element package ABAQUS, swelling elastomer specimen is modeled using 8-noded linear brick element with reduced integration (C3D8R). As mentioned in Chapter 3, Ogden hyper-elastic material model with second strain energy potential [19] is used for all simulations since it gives the best results [20]. Coefficients for the Ogden model are extracted from the experimental stress-strain data.

4.1 Simulation of compression test

Simulations for compression experiments are discussed in detail in Chapter 3. Stress-strain curves from these simulations are used here to determine the values of

Young's modulus. Simulations are conducted before swelling and after each swelling period (total one month period) under both salinity conditions, and for both materials. Specimen geometry before and after deformations is shown in **Figure 3**.

4.2 Simulation of bulk test

For bulk testing, elastomer disc is still under compression but restricted from any transverse deformations. Only the top surface can move downward (z-axis) under the compressive load as shown in the test setup in **Figure 2**. Simulation results are used to plot graphs of pressure against volumetric strain, for determination of bulk modulus through curve fitting. Deformed and undeformed specimens from bulk test simulation are shown in **Figure 4**.

5. Results and discussion: experimental

Results of the experimental investigation (mechanical and structural response of the elastomer to swelling) are discussed in this section. Variations in properties (volume, thickness, hardness, and density) due to swelling are discussed first. Later, results from compression and bulk experiments are presented and analyzed.

5.1 Swelling behavior

Effect of swelling on volume, thickness, hardness, and density of the two types of elastomer samples under different salinities is discussed below.

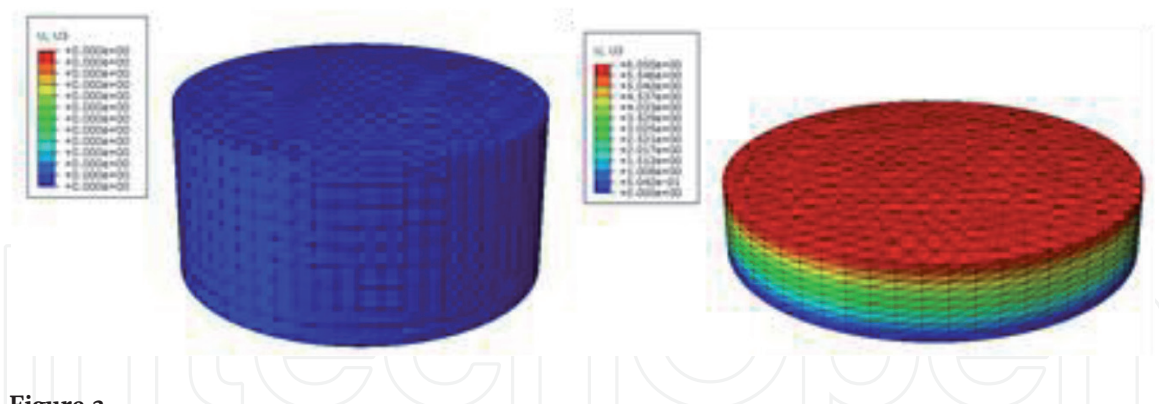


Figure 3.
Finite element model of compression test specimen; undeformed and deformed states.

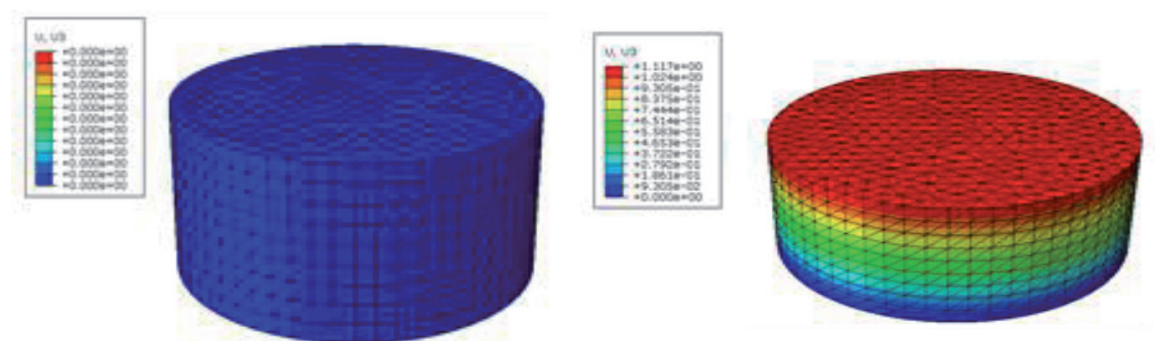


Figure 4.
Finite element model of bulk test specimen; undeformed and deformed states.

5.1.1 Volume change

Figure 5 shows the change in volume against days of swelling in 6000 ppm (0.6%) and 120,000 ppm (12%) brine solutions at 50°C for materials A and B. Both elastomers are of the fast-swell type, so increase in volume is very quick in the beginning, which can be observed in the first five days (reaching to almost one-third of total volume increase). More gradual increase was observed for the remaining one month period. As observed in earlier studies, swelling in lower-concentration salt-solution is higher than in higher-concentration brine due to existence of higher chemical potential gradient.

5.1.2 Thickness change

Figure 6 shows thickness change against swelling time for both materials. Fast swelling nature of the elastomer (materials A and B) results in more thickness increase in the beginning, and slower increase later on. Again, as expected, thickness swelling is higher for lower salt concentration.

5.1.3 Hardness change

Hardness keeps on decreasing as the elastomer swells more. **Figure 7** summarizes the change in hardness as samples for both materials swell in 0.6% and 12%

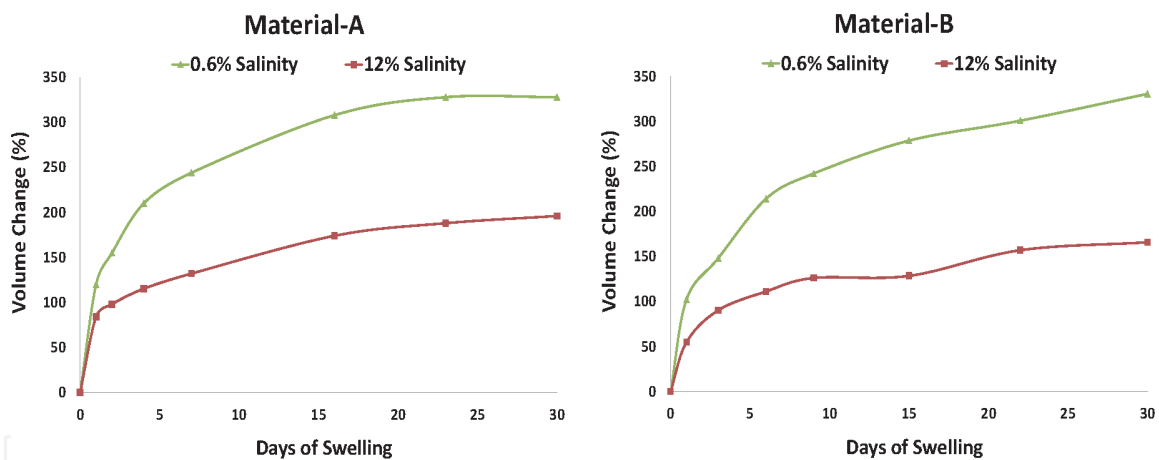


Figure 5.
Volume change in both materials in 0.6% and 12% salinity at 50°C.

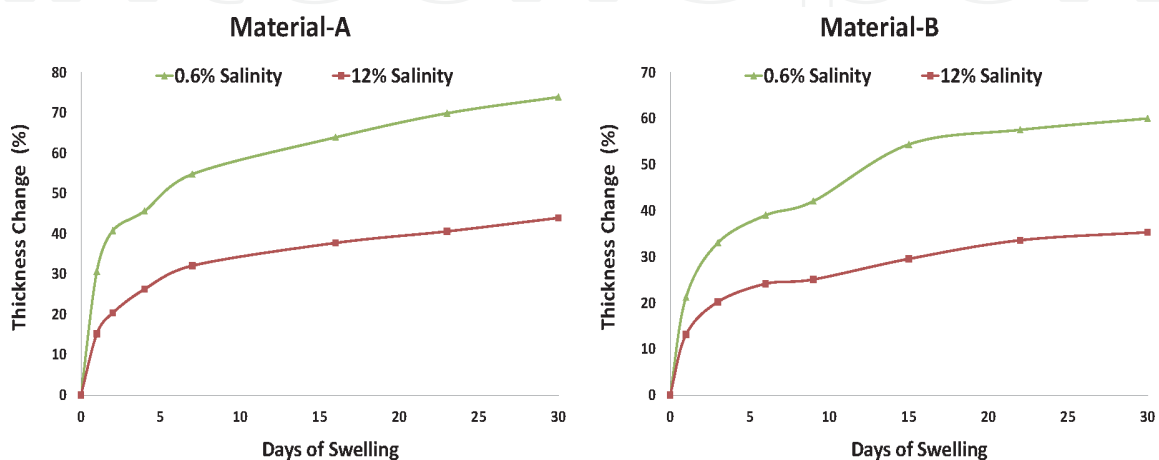


Figure 6.
Thickness change in both materials in 0.6% and 12% salinity at 50°C.

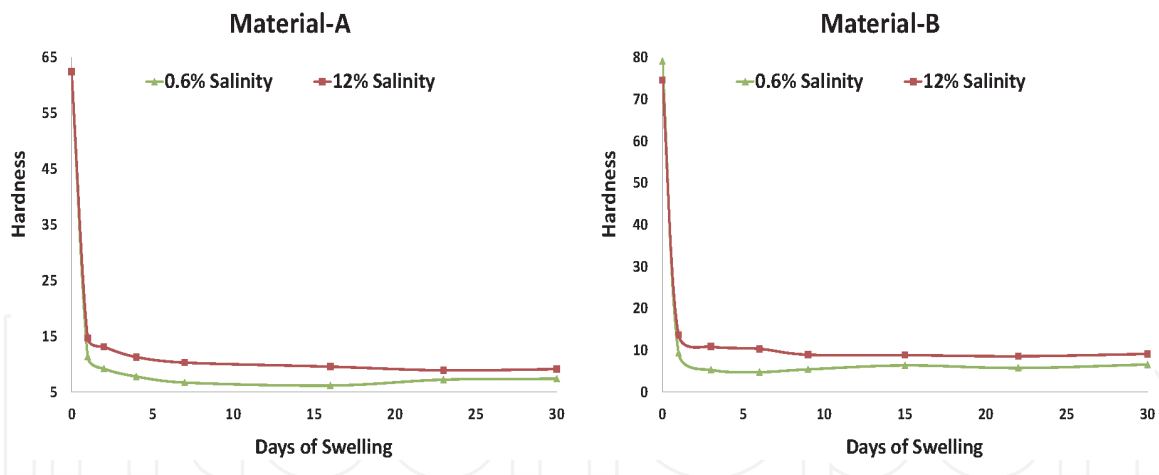


Figure 7.
Hardness change in both materials for 0.6% and 12% salinity at 50°C.

salt solutions, at 50°C. It is interesting to observe that within the first week of swelling, hardness drastically drops down, and then remains almost constant. Material *B* is harder in nature (unswelled hardness of about 75 shore-A as compared to 62 shore-A for material *A*). Hardness drop after swelling is more under 0.6% salinity solution for both materials.

In all of the above graphs, the overall trend is the same; very high swelling rate in the beginning, then a slow gradual change. This leads to a sharp initial drop in hardness, followed by almost no change for longer swelling periods. The slight fluctuating pattern may have roots in the nature of the swelling process [11, 21, 22]. Salt is one of the constituents of any swelling elastomer. When exposed to saline water, some salt can enter into the elastomer material (together with absorbed water), while some salt can break away from the elastomer and go into the salt solution. Rather than a consistent increase, this two-way salt transport cause slight fluctuations in the amount of swelling. Another important factor in swelling of such elastomers is the density of cross-link chains. Salt addition and breakaway can produce breaking and later re-forming of cross-link chains, causing increase or decrease of swelling at a particular time. As both these mechanisms are dependent on salt transport, fluctuation is more significant in higher concentration brine. After some time, a sort of equilibrium is reached, inflow and outflow of salt almost balancing out, and swelling starts to show a near steady-state behavior.

5.1.4 Density change

Density drops down considerably in the first few days for both materials and salinities, as can be seen in **Figure 8**. With more swelling, it increases a little before gradually dropping down to almost the same value as at the end of the first week. Due to the two-way water and salt transport during swelling of these elastomers, both volume and mass change at different rates; thus the slightly zigzag pattern of density variation.

5.2 Behavior under compressive loading

As an example, **Figure 9** shows 3-sample compressive stress–strain graphs for materials *A* and *B* in high salinity solution after four days of swelling. It can be seen that stress–strain behavior is non-linear in nature, as expected. It can also be observed that material *B* is more rigid than material *A*; thus the higher stresses and lower strains.

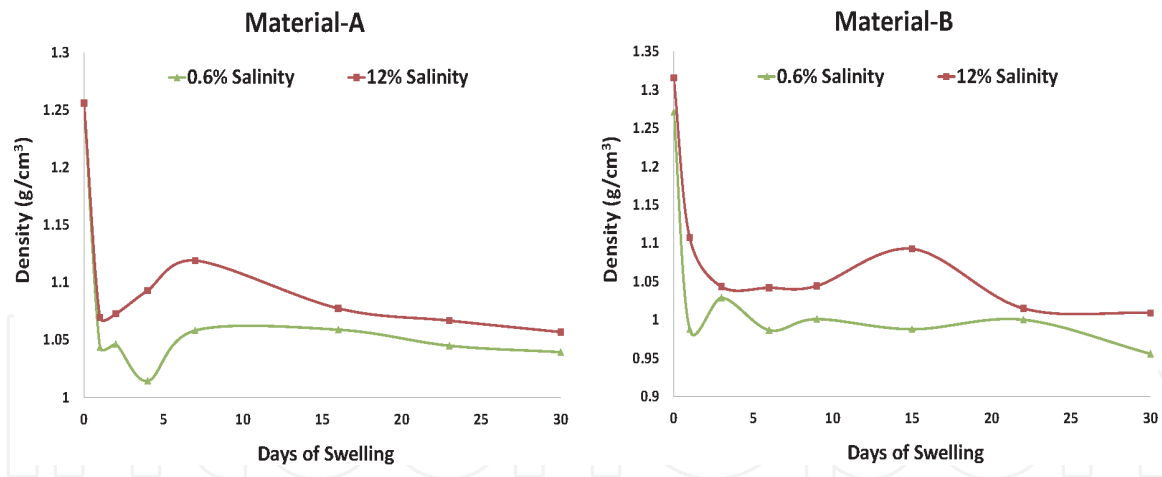


Figure 8.
Density variation in both materials for 0.6% and 12% salinity at 50°C.

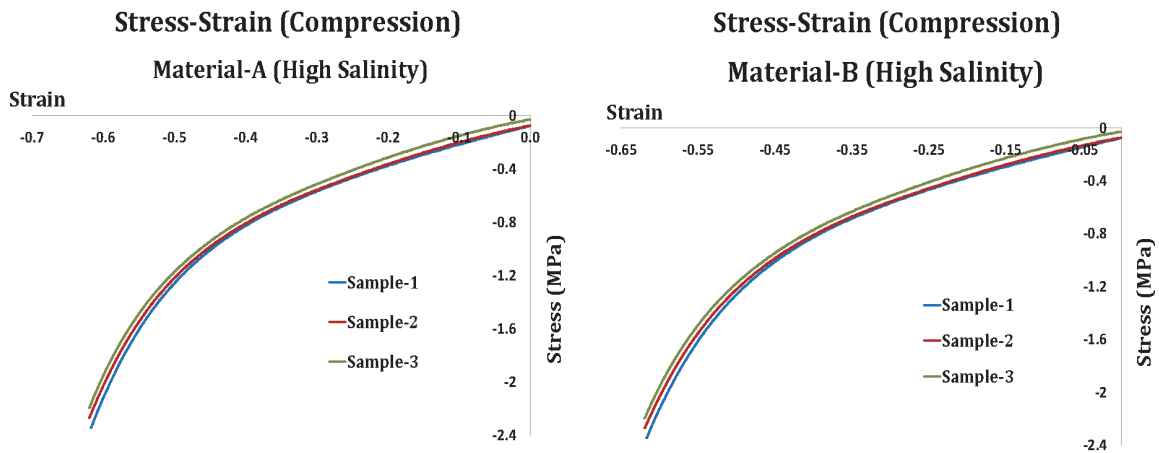


Figure 9.
Stress-strain graphs for both materials at 4 days of swelling; 3 samples.

Three-sample pressure-volumetric strain graphs for both elastomer types under high salinity after 23 days of swelling are shown in **Figure 10**. Though the overall behavior is still nonlinear, as expected for rubbers and elastomers, there is a significant linear portion. Bulk modulus is determined by fitting a straight line to the linear portion of these pressure-volumetric strain curves.

5.2.1 Mechanical and structural properties

At small strains (up to 10%), elastomers exhibit almost a linear stress-strain relationship and behave like other elastic materials [23]. Hence, for the extraction of Young's modulus, curve fitting is done on the initial 10% portion of the compressive stress-strain curve. For the determination of bulk modulus, some initial pressure-strain data is discarded before curve fitting. Elastomer disc does not touch the walls of the test cylinder at all points at the beginning of the test. As pressure is applied and the disc expands, it starts to fill this gap. Actual bulk test starts at the end of this gap-filling stage. Samples of linear curve fitting for extraction of elastic and bulk moduli (E and K) are shown in **Figure 11**. A very high goodness of fit of more than 99% is quite reassuring. Based on these values of E and K , shear modulus and Poisson's ratio are calculated using isotropic relations for elastic materials Eqs. (6) and (11). Chain density and average molecular weight are determined through polymer structure relations Eqs. (12) and (16).

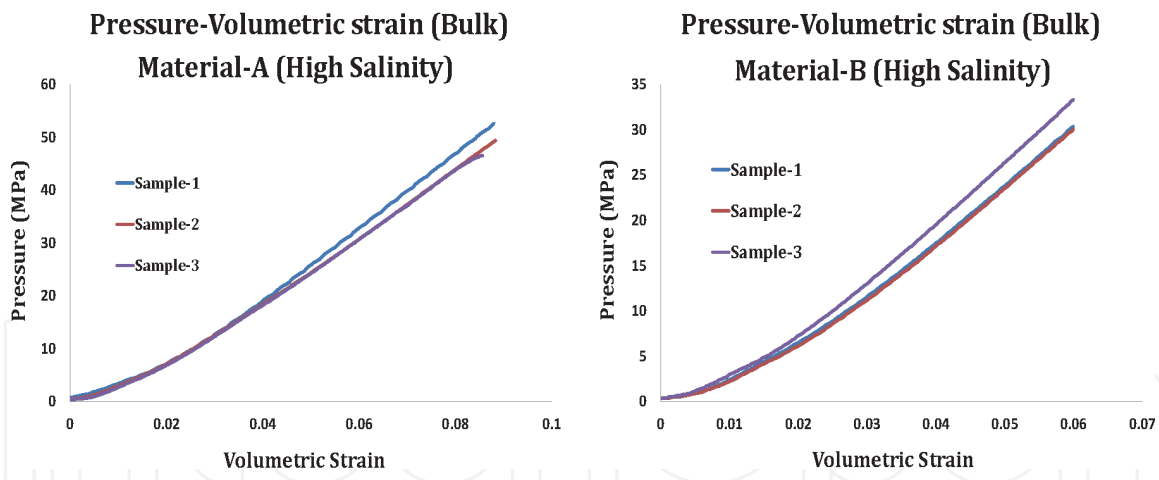


Figure 10. Three-sample pressure-strain (volumetric) curves for both materials for bulk test; 12% salinity; 23 days of swelling.

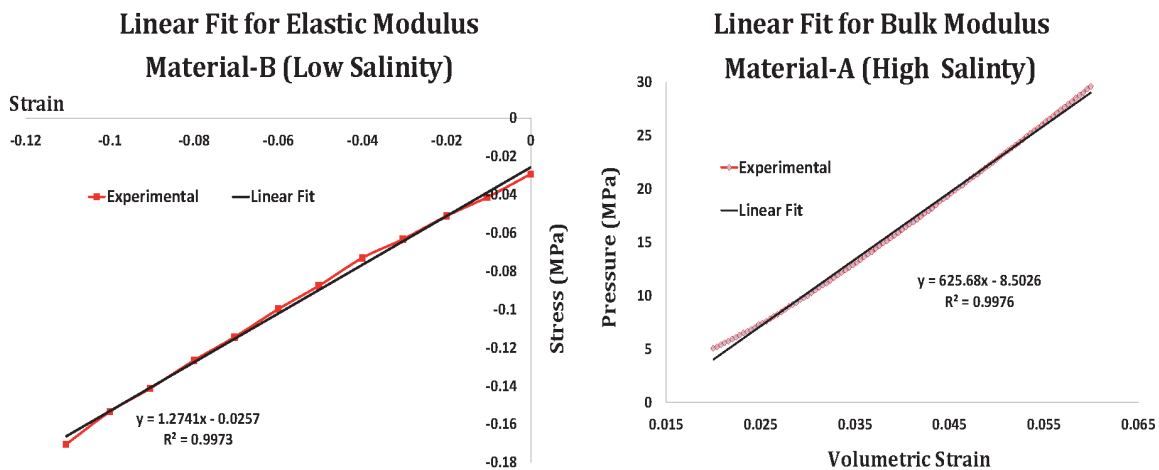


Figure 11. Linear curve fitting to experimental stress–strain data for determination of Young’s modulus (left), and pressure–volumetric strain for determination of bulk modulus (right).

5.2.2 Effect of swelling time

Compressive stress–strain behavior at different stages during the one month swelling period for materials A and B in high salinity brine is shown in **Figure 12**. Within a day of swelling, stress values drop by about 80–90% in both high and low salinities. Stress–strain curves after that are close to each other, the difference between curves for day-1 and day-30 not being very high. Lower stresses can be observed in low salinity solution for both materials, as expected; this is because high swelling is taking place in low salinity medium (as reported above), leading to softer samples. Also, strains after longer swelling periods are much larger. With more swelling, elastomer becomes softer, giving large strains at small loads, resulting in the trend shown in **Figures 9** and **10**.

Pressure–volumetric strain curves for one month period for both materials in low salinity are shown in **Figure 13**. A trend similar to the compression curves can be seen in these pressure–strain graphs also; larger drop in bulk modulus during the first few days of swelling, then more gradual. Reasons are the same as discussed above.

5.2.3 Variation of elastic Modulus

Variation of Young’s modulus (E) under compression for materials A and B under both salinities is shown in **Figure 14**. E -value decreases sharply in the first

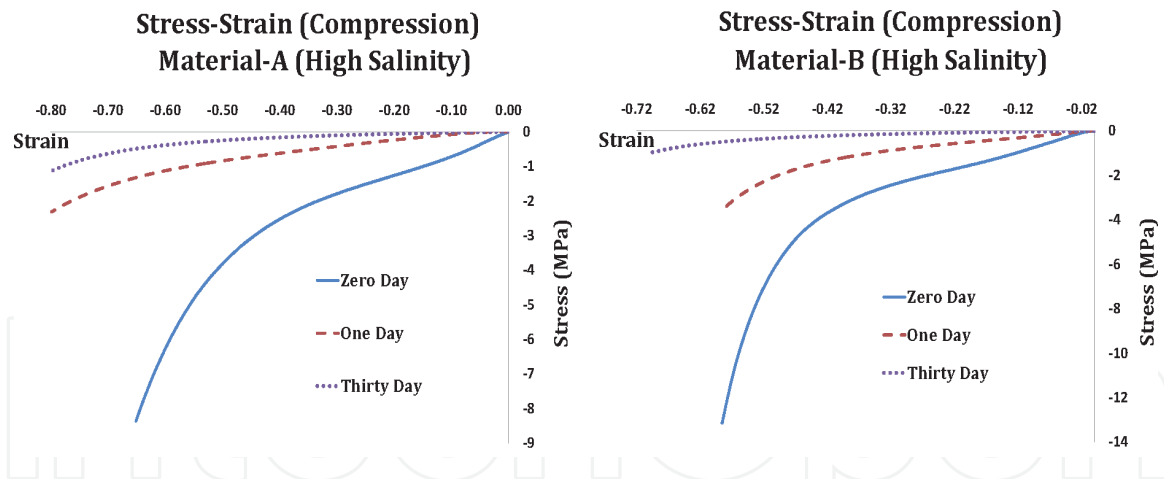


Figure 12.
Compressive stress–strain curves for both materials in high salinity for one month period.

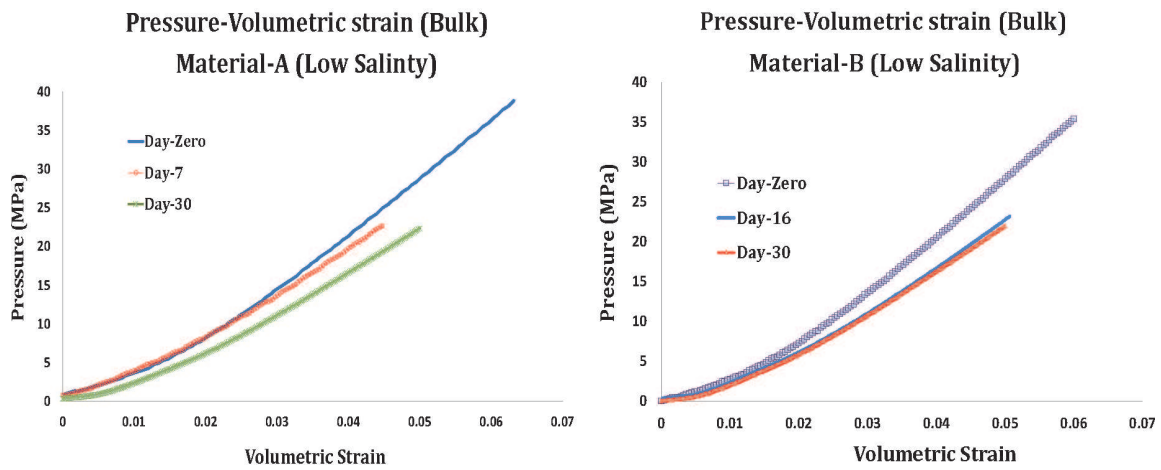


Figure 13.
Pressure-volumetric strain behavior before swelling and after 7 and 30 days of swelling in low salinity brine.

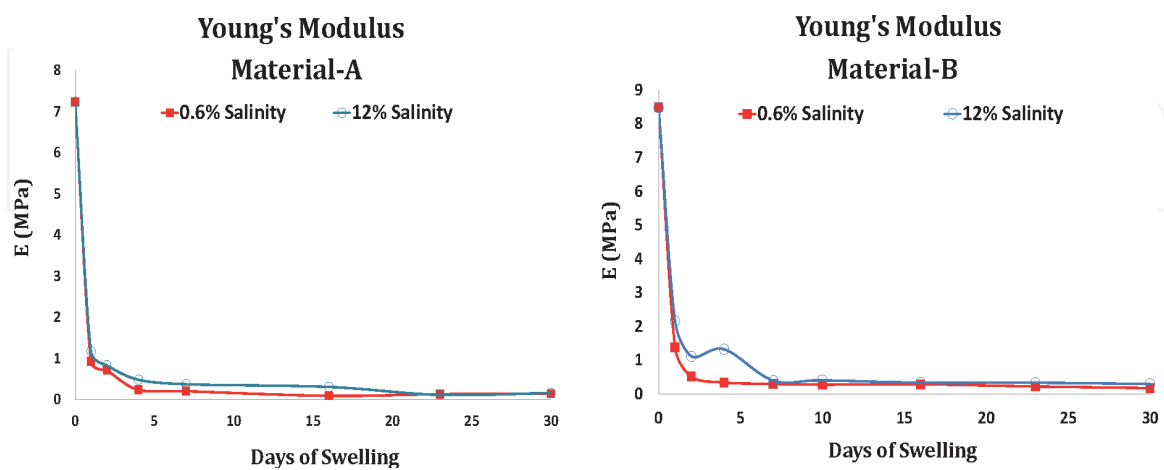


Figure 14.
Experimental results for Young's modulus for both materials.

few days (by almost 90%) and then becomes almost constant. This overall decreasing trend and slight fluctuation is due to the nature of swelling elastomers, as explained above. Modulus values for 12% salinity are slightly higher, as these samples are somewhat stiffer than the lower-salinity ones.

5.2.4 Variation of bulk Modulus

Variation of bulk modulus (K) over the 30-day swelling period for materials A and B under 0.6% and 12% salinities is shown in **Figure 15**. There is a notable fluctuation in the variation of K -value especially for material B; a sharp initial decrease, then a small increase, followed by a more gradual decrease to almost a constant value at the end of the one-month swelling period. Apart from the reasons for fluctuation discussed above, significant oscillation in K -value may also be rationalized from another perspective. During the compression test, sample elastomer disc is compressed in the axial direction, but is free to expand in the radial direction. However, in the bulk test, the disc specimen is constrained inside a cylinder so that there is uniaxial compression and no radial expansion. In effect, this violation of volume constancy means that the elastomer behavior changes from incompressible (compression test) to compressible (bulk test). This may lead to notable deviation from regular trends. As for salinity, the behavior is similar to that under compression; higher salinity gives larger values of bulk modulus.

5.2.5 Variation of Poisson's ratio

Variations of Poisson's ratio (ν) for both materials and both salinities exhibits a mirror behavior in comparison with elastic modulus, as shown in **Figure 16**. Poisson's ratio increases sharply in the first few days, and then becomes almost constant for the remaining swelling period. Again, lower salinity is giving higher values, as expected. For material B, there is some fluctuation during days 2 to 7 under 12% salinity. This variation pattern is similar to that of Young's modulus (**Figure 14**). As ν is dependent on E (isotropic relation), this fluctuation is expected. Moreover, it is interesting to note that ν approaches the limiting value of 0.5 within the first 10 days of swelling. This means that the assumption of incompressibility used in most analytical and numerical models of rubber-like materials is also justified for swelling elastomers, given a reasonably large swelling period.

5.2.6 Variation of shear Modulus

Variation of shear modulus (G) for both materials under low and high salinities is shown in **Figure 17**. Just like Young's modulus, value of shear modulus drops by more than 90% in the first 5 to 6 days, and then remains practically constant during the rest of the swelling period. Except for the first few days, both salinities show the

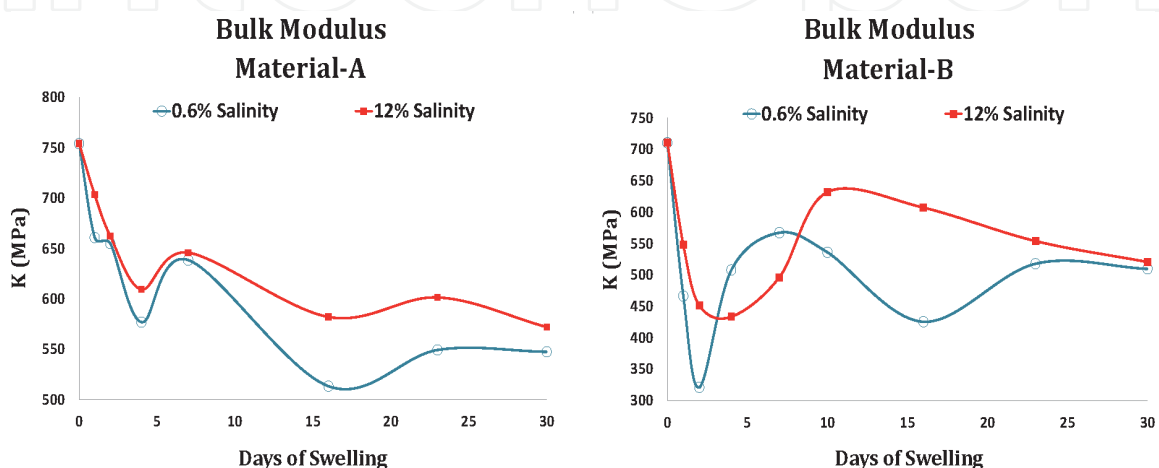


Figure 15.
Experimental results for bulk modulus for both materials.

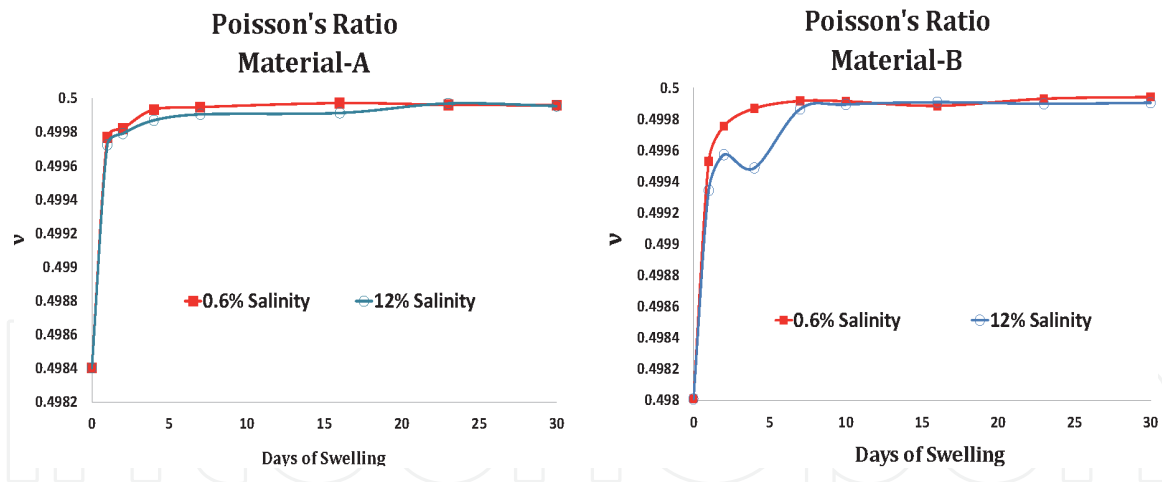


Figure 16.
Experimental results for Poisson's ratio for both materials.

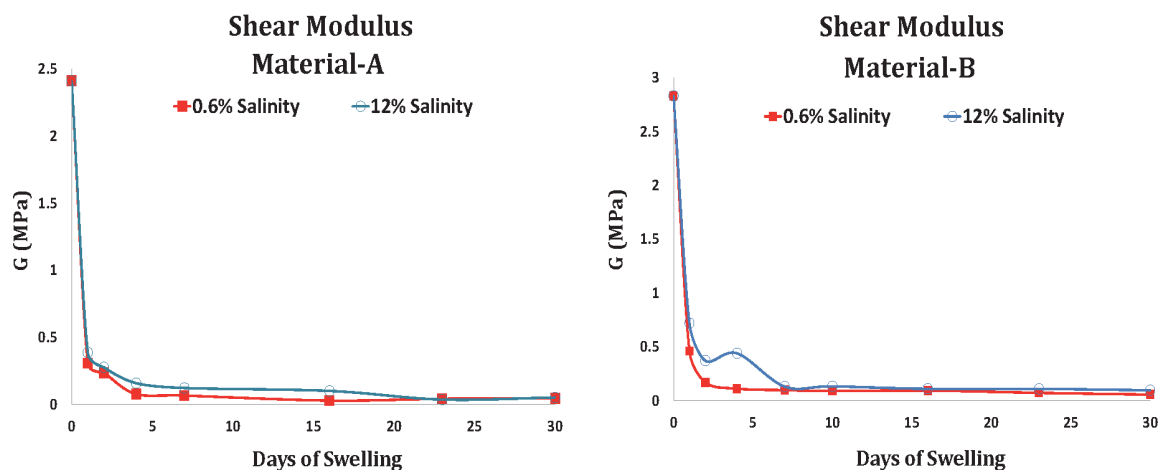


Figure 17.
Experimental results for shear modulus for both materials.

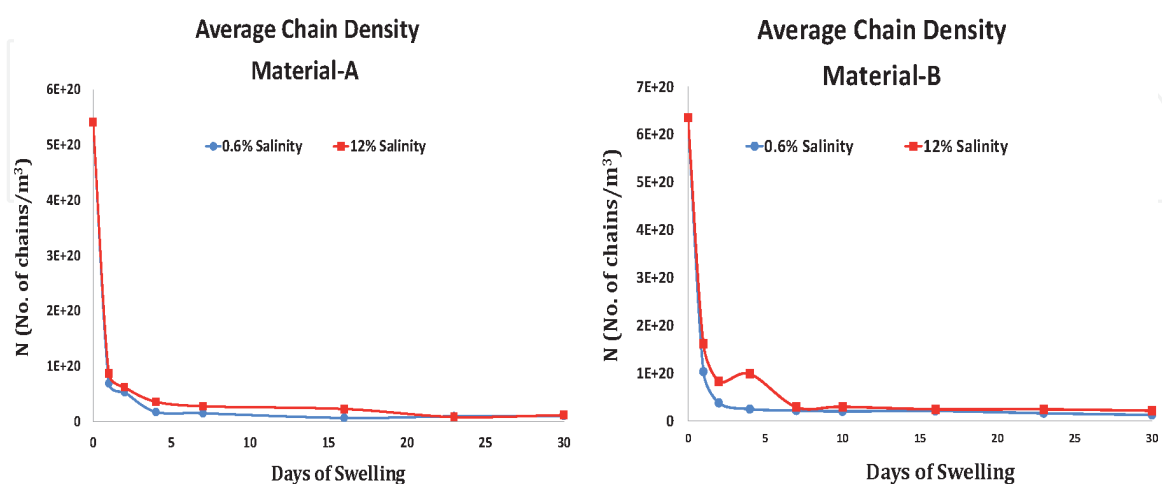


Figure 18.
Experimental results for average chain density for both materials.

same values. Some fluctuations for material B under 12% salinity can be observed during days 2 to 7. As G is related isotropically to E , it exhibits similar behavior as observed in Young's modulus.

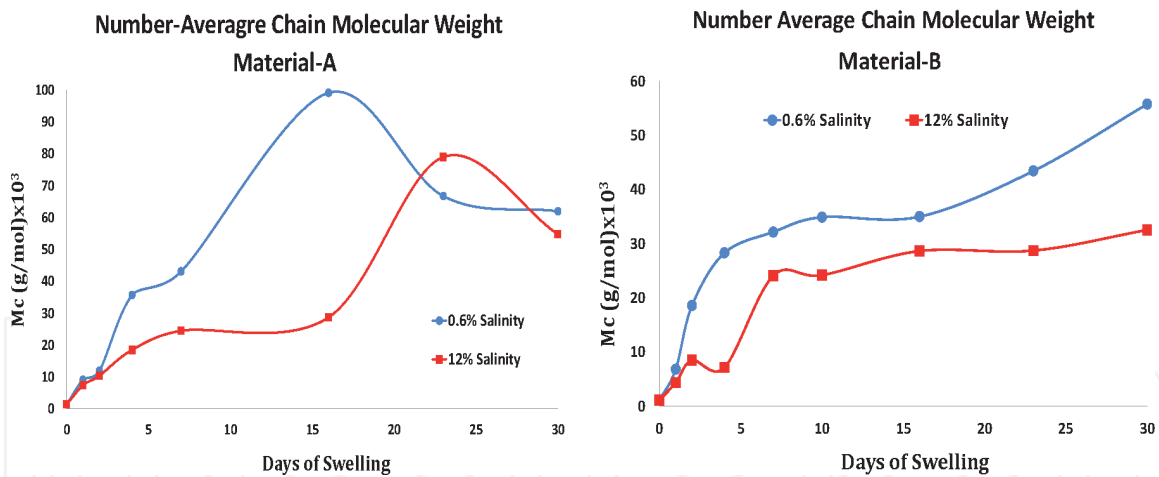


Figure 19. Experimental results for number-average chain molecular weight for both materials.

5.2.7 Variation of chain density

Variation in cross-link chain density (N) against amount of swelling is plotted in **Figure 18** for materials A and B in both salinities. Chain density drops drastically during the first few days, and then becomes nearly steady. During days 2 to 7, values are higher for material B in higher-salinity solution, otherwise response under both salinities is almost the same. As explained above, decrease in number of chains or cross-linking density occurs due to swelling, which makes the elastomer softer [11, 21, 22], thereby contributing to a decrease in stiffness, elastic modulus, and rigidity (shear modulus). This change in polymer structure due to swelling is a direct explanation of the variation pattern observed in the mechanical properties.

5.2.8 Variation of molecular weight

Figure 19 shows the variation in number-average chain molecular weight (M_c) against swelling time over the 30-day test period for materials A and B in both salinities. There is an overall increasing behavior with higher swelling amount, but with a somewhat fluctuating pattern, material A exhibiting higher fluctuations. The various reasons discussed above (including two-way transport of salt, forming and breaking of cross-link chains, etc) are equally applicable in explanation of the observed variation in average molecular weight. On top of that, M_c is related to both density and shear modulus, so it is exhibiting the combined effect of two fluctuations.

Slight fluctuations during the first week of swelling in the values of material and structural properties studied are due to this two-pronged variation in swelling amount. Compared to bulk tests, fluctuation is almost insignificant in compression tests due to the simple uniaxial nature of the load applied. *As significant variation in material properties occurs only in the first 10 days, these values can serve as reasonable design properties for future applications, removing the need for material testing beyond 10 days of swelling.*

6. Results and discussion: numerical

Stress-strain curves under compressive loading, and pressure-strain curves for bulk testing are also produced through numerical simulation, using Ogden

hyperelastic material model with second-degree strain energy function ($N = 2$). Graphs for variation of mechanical properties against swelling are generated from the numerical results. This work has been done for both materials under both salinities for the entire one-month swelling period. However, only a few representative graphs are presented below for comparison of experimental and numerical results.

6.1 Behavior under compressive loading

Stress-strain plots in the 10% strain region for experimental and numerical results of compression test for material B under 12% salinity are shown in **Figure 20**, before swelling, and after one day of swelling. Variation of pressure against volumetric strain (experimental and numerical) from bulk test results of material B under 0.6% salinity is given in **Figure 21**. Though variation trends are roughly the same, there is considerable difference between experimental and numerical curves in general.

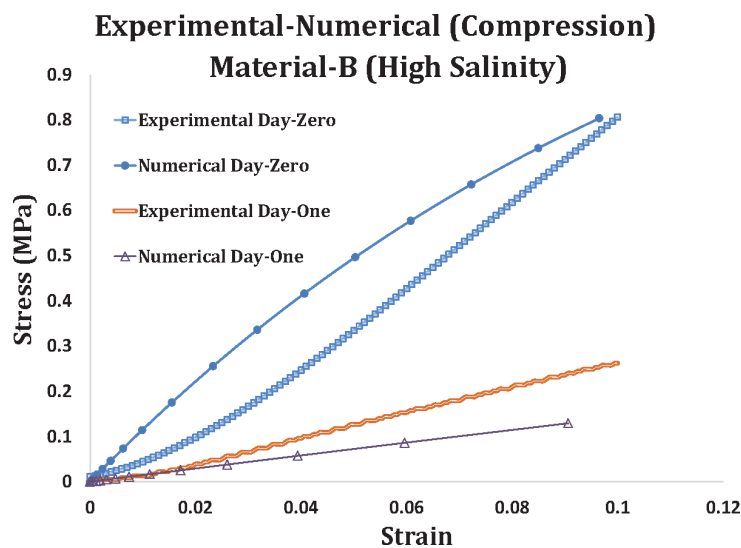


Figure 20. Comparison of experimental and numerical (Ogden; $N = 2$) results for compression test for both materials, before swelling (day zero) and after one-day of swelling.

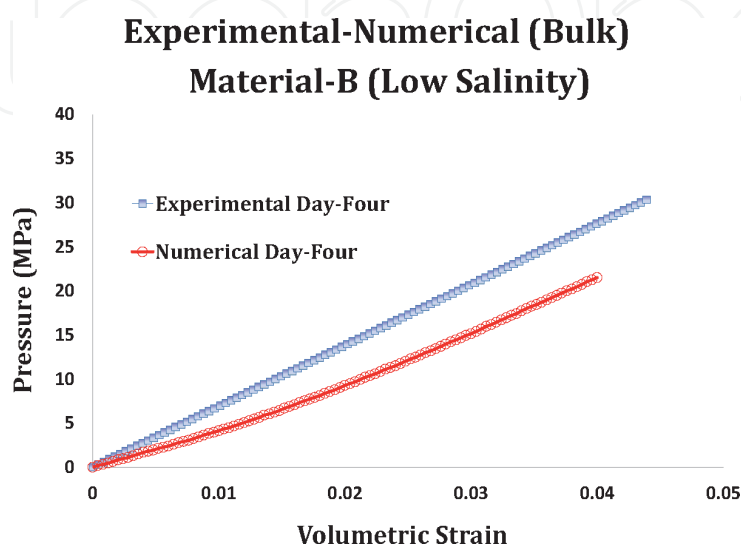


Figure 21. Comparison of experimental and numerical (Ogden; $N = 2$) results for bulk test for material B in low salinity after 4 days of swelling.

6.1.1 Mechanical properties

Variation of Young's modulus, Poisson's ratio, and shear modulus for the two materials under 0.6% and 12% salinity over the 30-day swelling period is shown in **Figures 22–24**. A reasonable match between experimental and simulation results can be observed. There are notable differences during days 2 to 7, especially in the case of higher salinity (12%), but the curves come close to each other upon further swelling.

Comparison between experimental and numerical results for bulk tests is given in **Figures 25 and 26**, for materials *A* and *B* respectively. Numerical results are seriously different from experimental ones in all cases over the 30-day swelling period. Even in the experimental results, there is serious fluctuation in bulk modulus, as observed and discussed earlier in Section 4. On top of that, it is well known that the available hyperelastic models are based on shear deformation theory, and do not include the effect of bulk deformation. This would obviously imply a notable difference in experimental and simulation results of bulk behavior.

6.1.2 Note

As discussed in detail in Chapter 6, Ogden model ($N = 2$) is the best one among the available hyperelastic models for representation of swelling elastomers.

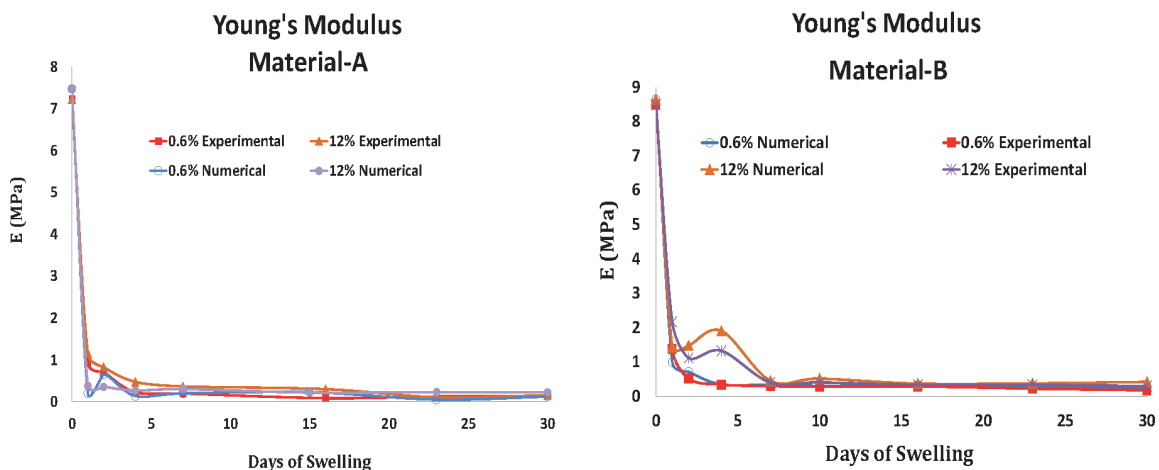


Figure 22.
 Comparison of experimental and numerical results for variation of Young's modulus.

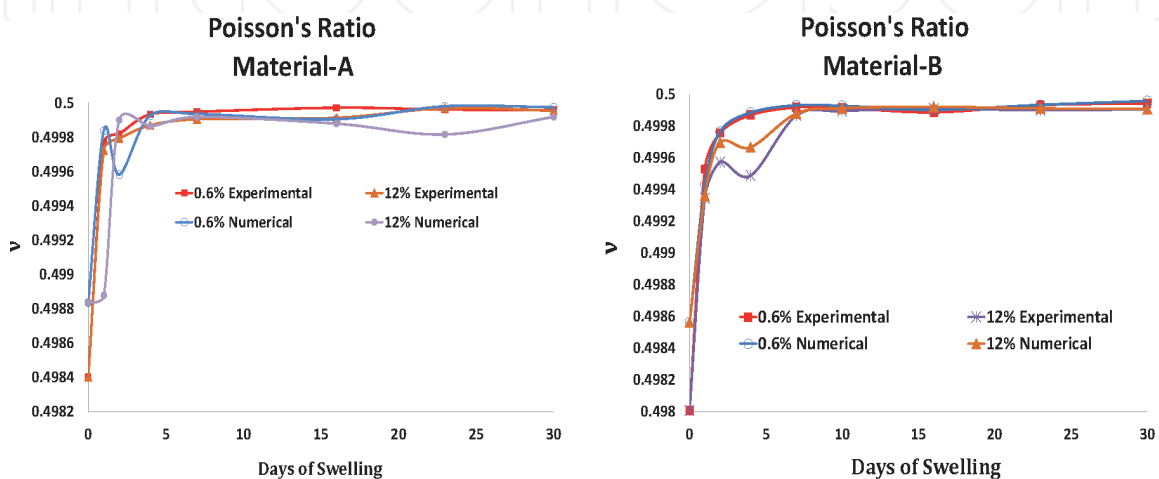


Figure 23.
 Comparison of experimental and numerical results for variation of Poisson's ratio.

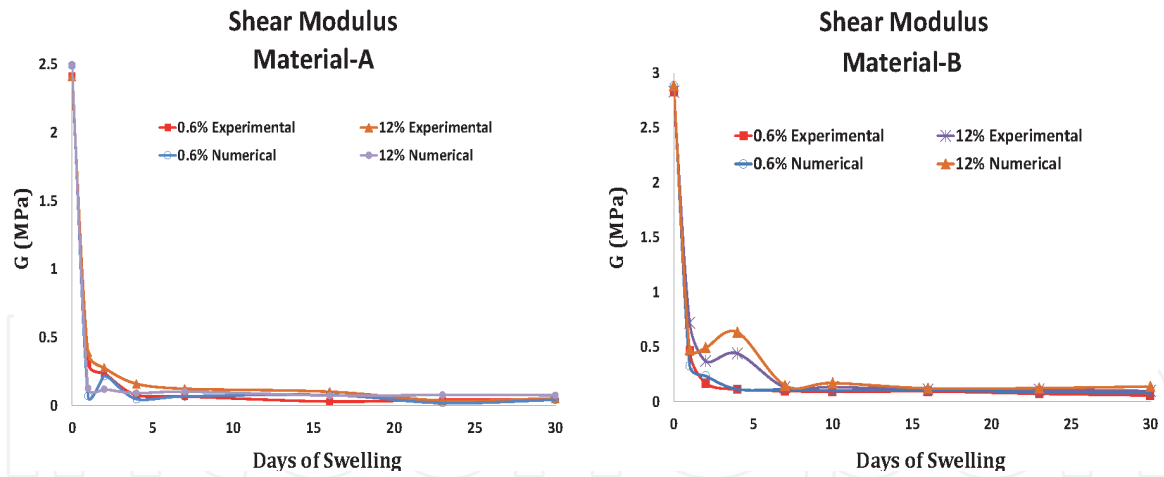


Figure 24. Comparison of experimental and numerical results for variation of shear modulus.

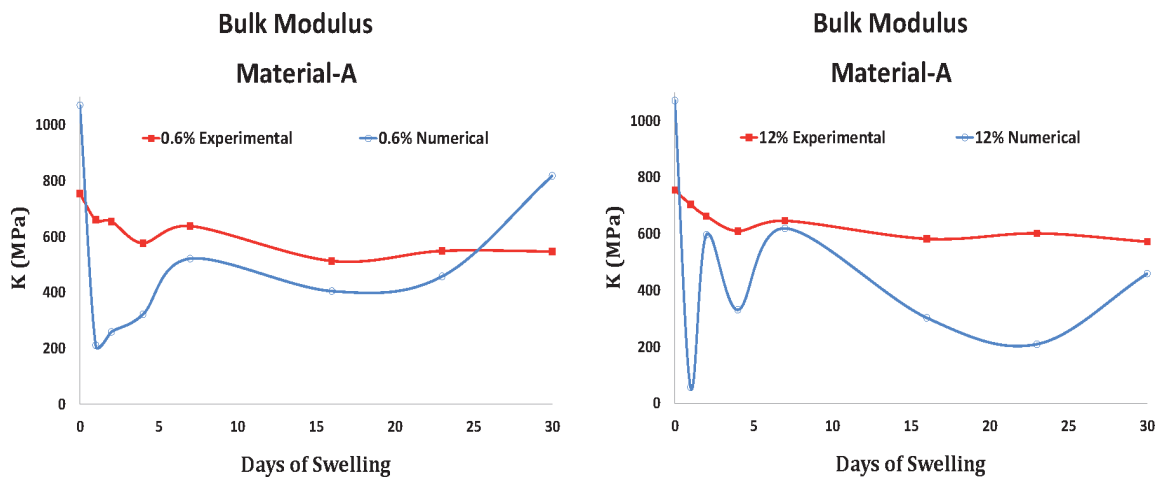


Figure 25. Comparison of experimental and numerical results for variation of bulk modulus for material A.

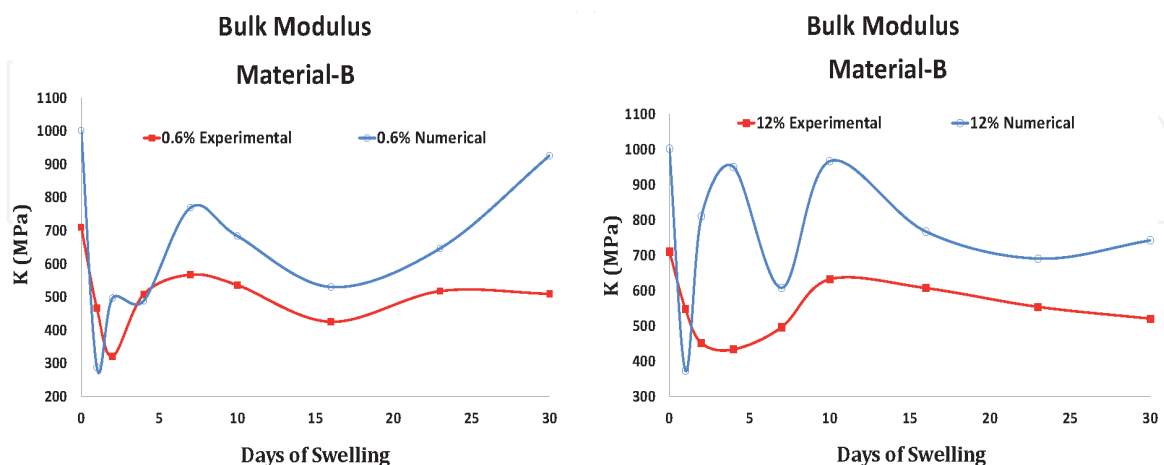


Figure 26. Comparison of experimental and numerical results for variation of bulk modulus for material B.

However, as most of the graphs in this section show, even the Ogden model does not yield results that follow experimental ones closely. In the absence of any other model, this may be the only choice for numerical simulation, but it is not good enough. *This highlights the need for a new material model that can more closely*

capture the actual behavior of swelling elastomers. As described later in Chapter 11, this new model should include continuum mechanics, diffusion, and thermodynamics of mixing to account for large deformations in the case of swelling.

7. Conclusions

Experimental and numerical investigation of changes in compressive and bulk behavior of two water-swelling elastomers has been presented. Tests were carried out on standard compression and bulk samples (following ASTM standards) before swelling and after different swelling periods. Elastic modulus and bulk modulus were experimentally determined under different swelling conditions. Shear modulus and Poisson's ratio were estimated using isotropic relations. Cross-link chain density and number average molecular weight were obtained using predictive equations of polymer structure. Mechanical testing was also modeled and simulated using the nonlinear finite element package ABAQUS, using Ogden hyperelastic model with second strain energy potential. Simulation results are somewhat close to experimental ones in most of the cases. However, there are significant differences in various other situations. This strengthens the need for a new material model to more effectively represent the behavior of swelling elastomers.

Author details

Sayyad Zahid Qamar^{1*}, Maaz Akhtar² and Tasneem Pervez¹

1 Mechanical and Industrial Engineering Department, Sultan Qaboos University, Muscat, Oman

2 Mechanical Engineering Department, N.E.D. University of Engineering and Technology, Karachi, Pakistan

*Address all correspondence to: sayyad@squ.edu.om

IntechOpen

© 2021 The Author(s). Licensee IntechOpen. Distributed under the terms of the Creative Commons Attribution - NonCommercial 4.0 License (<https://creativecommons.org/licenses/by-nc/4.0/>), which permits use, distribution and reproduction for non-commercial purposes, provided the original is properly cited. 

References

- [1] Polgar LM, Fallani F, Cuijpers J, Raffa P, Broekhuis AA, van Duin M, Picchioni F (2017) "Water-Swellable Elastomers: Synthesis, Properties and Applications," *Reviews in Chemical Engineering*, 35 (1), p 45-72
- [2] Al-Douserri K, Barnes C, Young D, Smith P (2010) "Swellable Packers Provide a Brown Field Water Management Solution in Open and Cased Hole, SPE Oil and Gas India Conference and Exhibition (OGIC), Mumbai, India.
- [3] Ekpe J, Kompantsev A, Al-Thuwaini J, Belousov Y, Ashoor A, Abdul-Aziz ME (2011) "First Multi-Stage Swell Packers Open Hole Completion in Rub Al-Khali Empty Desert: Case Study," Paper # SPE 142523, SPE Middle East Unconventional Gas Conference and Exhibition, Muscat, Oman
- [4] Kennedy GP, Lawless AR, Shaikh AK, Alabi IB (2005) "The Use of Swell Packers as a Replacement and Alternative to Cementing," Paper # SPE 95713, SPE Annual Technical Conference and Exhibition, Dallas, Texas
- [5] Keshka A, Elbarbay A, Menasria C, Smith P (2007) "Practical Uses of Swellable Packer Technology to Reduce Water Cut: Case Studies from the Middle East and other Areas," Paper # SPE 108613, Offshore Europe, Scotland, UK
- [6] Kleverlaan M, van Noort RH, Jones I (2005) "Deployment of Swelling Elastomer Packers in Shell E&P," Paper # SPE/IADC 92346, SPE/IADC Drilling Conference, Amsterdam, Netherlands
- [7] Chen X, Bartos J, Salem H, Zonoz R (2016) "Elastomers for High Pressure Low Temperature HPLT Sealing," Paper # IDOTC-27227, Offshore Technology Conference, 2-5 May 2016, Houston, Texas, USA
- [8] Ojha K, Saxena A, Pathak AK (2014) "Underbalanced Drilling and Its Advancements: An Overview," *Journal of Petroleum Engineering and Technology*, Vol 4, No 2
- [9] Patel H, Salehi S, Ahmed R, Teodoriu C (2019) "Review of Elastomer Seal Assemblies in Oil and Gas Wells: Performance Evaluation, Failure Mechanisms, and Gaps in Industry Standards," *Journal of Petroleum Science and Engineering*, 179 (2019), p 1046-1062
- [10] Al-Yami AS, Nasr-El-Din HA, Awang MZB, Al-Humaidi AS, Al-Arfaj MK (2008) "Swelling Packers; Lab Testing and Field Application," Paper # IPTC 11997, International Petroleum Technology Conference. Kuala Lumpur, Malaysia
- [11] Qamar SZ, Al-Hiddabi SA, Pervez T, Marketz F (2009) "Mechanical Testing and Characterization of a Swelling Elastomer," *Journal of Elastomers and Plastics*, 41 (5), p 415-431
- [12] Qamar SZ, Akhtar M, Pervez T, Al-Kharusi MSM (2013) "Mechanical and Structural Behavior of a Swelling Elastomer under Compressive Loading," *Materials and Design*, 45 (March 2013), p 487-496
- [13] ABAQUS (2012) Software version 6.11, Dassault systems
- [14] Hosford WF (2010) *Mechanical Behavior of Materials*, Cambridge University Press
- [15] Hibbeler RC (2016), *Mechanics of Materials*, 10th edition, Pearson
- [16] Gent AN (2012) *Engineering with Rubbers: How to Design Rubber Components*, Carl Hanser Verlag Publishers, Munich, Germany

[17] Treloar LRG (2005) *The Physics of Rubber Elasticity*, Oxford University Press, Oxford

[18] ASTM D575–91 (2007) “Standard Test Methods for Rubber Properties in Compression,” American Society for Testing and Materials

[19] Ogden R (1972) “Large Deformation Isotropic Elasticity — On the Correlation of Theory and Experiment for Incompressible Rubberlike Solids,” *Proceedings of the Royal Society of London. A. Mathematical and Physical Sciences*, 326(1567), 565-584.

[20] Akhtar M, Qamar SZ, Pervez T, Khan R, Al-Kharusi MSM (2012) “Elastomer Seals in Cold Expansion of Petroleum Tubulars: Comparison of Material Models,” *Materials and Manufacturing Processes*, 27(7), p 715-720

[21] Qamar SZ, Pervez T, Akhtar M (2016) “Performance Evaluation of Water-Swelling and Oil-Swelling Elastomers,” *Journal of Elastomers and Plastics*, 48 (6) 2016, p 535-545

[22] Qamar SZ, Pervez T, Akhtar M, Al-Kharusi MSM (2012) “Design and Manufacture of Swell Packers: Influence of Material Behavior,” *Materials and Manufacturing Processes*, 27 (7), p 721-726

[23] Gent A (1996) “A New Constitutive Relation for Rubber,” *Rubber Chemistry and Technology*, 69(1), 59-61.